Monthly Notices
of the
ROYAL ASTRONOMICAL SOCIETY

MNRAS **461,** 1023–1031 (2016)
Advance Access publication 2016 June 8

doi:10.1093/mnras/stw1372

Brownian motion of massive black hole binaries and the final parsec problem

E. Bortolas,[1,2★] A. Gualandris,[3] M. Dotti,[4,5] M. Spera[1] and M. Mapelli[1,5]

[1]*INAF, Osservatorio Astronomico di Padova, Vicolo dell'Osservatorio 5, I-35122 Padova, Italy*
[2]*Dipartimento di Fisica e Astronomia 'Galileo Galilei', Università di Padova, Vicolo dell'Osservatorio 3, I-35122 Padova, Italy*
[3]*Department of Physics, University of Surrey, Guildford GU2 7XH, UK*
[4]*Dipartimento di Fisica G. Occhialini, Università degli Studi di Milano, Bicocca, Piazza della Scienza 3, I-20126 Milano, Italy*
[5]*INFN, Sezione di Milano-Bicocca, Piazza della Scienza 3, I-20126 Milano, Italy*

Accepted 2016 June 3. Received 2016 June 1; in original form 2016 April 29

ABSTRACT

Massive black hole binaries (BHBs) are expected to be one of the most powerful sources of gravitational waves in the frequency range of the pulsar timing array and of forthcoming space-borne detectors. They are believed to form in the final stages of galaxy mergers, and then harden by slingshot ejections of passing stars. However, evolution via the slingshot mechanism may be ineffective if the reservoir of interacting stars is not readily replenished, and the binary shrinking may come to a halt at roughly a parsec separation. Recent simulations suggest that the departure from spherical symmetry, naturally produced in merger remnants, leads to efficient loss cone refilling, preventing the binary from stalling. However, current *N*-body simulations able to accurately follow the evolution of BHBs are limited to very modest particle numbers. Brownian motion may artificially enhance the loss cone refilling rate in low-*N* simulations, where the binary encounters a larger population of stars due its random motion. Here we study the significance of Brownian motion of BHBs in merger remnants in the context of the final parsec problem. We simulate mergers with various particle numbers (from 8k to 1M) and with several density profiles. Moreover, we compare simulations where the BHB is fixed at the centre of the merger remnant with simulations where the BHB is free to random walk. We find that Brownian motion does not significantly affect the evolution of BHBs in simulations with particle numbers in excess of one million, and that the hardening measured in merger simulations is due to collisionless loss cone refilling.

Key words: black hole physics – galaxies: kinematics and dynamics – galaxies: nuclei.

1 INTRODUCTION

Astrophysical observations suggest that massive black holes (MBHs) with masses in the range 10^6–10^{10} $M_\odot$ inhabit a large fraction of galactic nuclei, and their presence in most massive galaxies is suspected to be ubiquitous (e.g. Ferrarese & Ford 2005). In addition, according to the ΛCDM cosmological model, galaxies grow through the agglomeration of smaller structures, at least some of which contain a black hole seed at early times.[1] Therefore BHBs may form in large numbers along cosmic time, as a result of galaxy mergers.

The formation and evolution of BHBs has received considerable attention in the last years, as the merger and final coalescence of MBH pairs is expected to represent the loudest source of gravitational waves (GWs) in the 10^{-4}–10^{-1} Hz band (Thorne & Braginskii 1976). These low-frequency signals cannot be observed by ground-based interferometers like LIGO and VIRGO, which have recently detected the first ever GW waveform from the coalescence of two stellar mass black holes (Abbott et al. 2016). However, the lower mass MBH mergers will be accessible to the new generation of space-based gravity interferometers, such as *eLISA*, the straw-man mission of *The Gravitational Universe* theme, selected by *ESA* for L3 (eLISA Consortium 2013). The most massive BHBs, on the other hand, can be detected by the Pulsar Timing Array (Babak et al. 2016) which is already operational and using the very accurate timings of pulsars to observe GWs. The detection of low-frequency GWs from MBHs would provide crucial information on the masses

★E-mail: elisa.bortolas@oapd.inaf.it

[1]As can be inferred by the fact that galaxies turn on as active galactic nuclei for a small fraction of their lifespan (Haehnelt & Rees 1993).

and spins of MBHs and on the merger rate of BHBs, which would allow to constrain models of their formation and growth (Volonteri 2010). However, the coalescence of BHBs has been put under scrutiny in the past years due to theoretical arguments on loss cone refilling (e.g. Begelman, Blandford & Rees 1980) and N-body simulations of BHB pairing in isolated spherical galaxies (e.g. Makino & Funato 2004), both hinting at a possible stalling of the BHBs at $\sim$1 pc scales, an issue commonly referred to as the 'Final Parsec Problem'.

The path to coalescence of a BHB in gas-poor galaxies can be divided into three main phases (Begelman et al. 1980): (i) a first phase during which dynamical friction drags the MBHs towards the centre of the merger remnant; (ii) a second phase in which subsequent binary shrinking is induced by three-body interactions between the BHB and the surrounding stars (the so-called *slingshot mechanism*), leading to the ejection of stars from the centre of the remnant (Saslaw, Valtonen & Aarseth 1974); (iii) a third phase of evolution characterized by either stalling at roughly a parsec separation or inspiral due to GW emission followed by coalescence to a single MBH. While the transition from the dynamical friction to the slingshot phase is quick for any realistic MBH masses, the efficiency of gravitational slingshot interactions drops after roughly a dynamical time, when the population of stars on initially low-angular momentum orbits has been ejected by the binary, possibly leading to stalling. The fate of the BHB at this stage depends crucially on the supply of stars in the *loss cone*, i.e. the low angular momentum region of the phase space harbouring stars that can experience an interaction with the binary (Begelman et al. 1980; Yu 2002; Milosavljević & Merritt 2003).

In principle, two-body relaxation always contributes to loss cone refilling via star scatterings, however it operates on a time-scale that strongly depends on the number N of particles in the system (roughly $T_{\rm r} \propto N/\log N$), and this exceeds the age of the Universe in almost all sufficiently luminous galaxies (i.e. galaxies harbouring MBHs with masses in excess of $10^7\,{\rm M}_\odot$). Consequently, relaxation-induced loss cone refilling is generally assumed to be ineffective, and the binary would not be able to reach the GW inspiral phase in a Hubble time. Direct-summation N-body simulations of BHB inspiral in spherical stellar environments confirm the stalling and the dependence on particle number (Makino & Funato 2004; Berczik, Merritt & Spurzem 2005; Merritt, Mikkola & Szell 2007b). Simulations show a completely different behaviour, though, when the merger of two galaxies hosting a central MBH is followed from early times (Khan, Just & Merritt 2011; Preto et al. 2011; Gualandris & Merritt 2012). BHBs formed during mergers are able to continue hardening well after the first central depletion, which implies that the loss cone is efficiently replenished at all times. Because merger remnants are typically non-spherical, the sustained binary hardening is attributed to the population of centrophilic orbits unique to non-spherical potentials. In these cases, BHB coalescence can be reached in a few Gyr at the most. Collisionless loss cone refilling has been confirmed as the driver of BHB evolution in simulations of binaries evolving in isolated triaxial galaxies (Vasiliev, Antonini & Merritt 2015, Gualandris et al., in preparation), in which collisional refilling is reduced or eliminated by using a different numerical technique and increasing particle number significantly.

However, particle numbers representative of real galaxies remain unachievable by N-body simulations and, unless collisional relaxation is eliminated in some way, loss cone refilling due to two-body relaxation cannot be avoided. This is particularly true for direct-summation methods, which are needed when one wishes to model the detailed evolution of the BHB, but whose N^2 computational complexity limits applicability to a few million particles at most.

Simulations with low N might be plagued by an increased Brownian motion of the binary's centre of mass (CoM). Whenever a slingshot interaction occurs, the binary CoM experiences a recoil whose amplitude depends on the mass of the ejected star. In low-N models, where stars are orders of magnitude more massive than in real galaxies, the binary experiences an enhanced Brownian motion. As it wanders within its typical Brownian radius, the binary can intersect more stars than it would were it confined to a smaller region. Therefore, the loss cone is artificially enhanced.

What is the importance of Brownian motion and whether it depends on the resolution has been debated for a long time. It has been argued that *'a substantial fraction of all massive binaries in galaxies can coalesce within a Hubble time'* due to the effects of Brownian motion (Chatterjee, Hernquist & Loeb 2003). In contrast, other theoretical studies suggest that Brownian motion is modest for BHBs in real galactic nuclei (Merritt 2001; Milosavljević & Merritt 2003), but it remains to be established whether it is responsible for the sustained hardening of BHBs observed in direct-summation merger simulations. Here we study the Brownian motion of BHBs in merger simulations and its connection with loss cone repopulation and the final parsec problem.

We performed a suite of direct-summation N-body simulations of the merger of two spherical gas-free galaxies containing an MBH in the centre. We measure the wandering of the BHB that forms and its hardening rate and show that the Brownian motion does not significantly affect the binary evolution at large particle numbers. In order to draw a more robust conclusion, we perform additional simulations in which we artificially anchor the binary's CoM to the centre of the density cusp as the system evolves. We find that the binary shrinking rate in these simulations is in good agreement with the one found in the free-binary case when the resolution (i.e. particle number) of our simulations is maximal. This allow us to completely rule out the possibility of a spurious wandering-induced loss cone refilling in simulations with N in excess of one million.

The paper is organized as follows: Section 2 details the numerical methods and initial conditions adopted; Section 3 presents results of the BHB evolution, while we discuss Brownian motion and its dependence on resolution in Section 4; finally, in Section 5 we present a summary and conclusions.

2 METHODS

We performed a suite of direct-summation N-body simulations of equal mass galaxy mergers, varying the resolution (i.e. particle number N) and the density distribution of the progenitor galaxies. Each galaxy follows a Dehnen's density profile (Dehnen 1993):

$$\rho(r) = \frac{(3-\gamma)\,M_{\rm g}}{4\pi}\frac{r_0}{r^{\gamma}(r+r_0)^{4-\gamma}}, \qquad (1)$$

with total mass $M_{\rm g}$, scale radius r_0 and inner slope γ. Two different realisations of the same model were placed on a bound elliptical orbit in the $x-y$ plane, with initial orbital eccentricity $e = 0.5$, separation $\Delta r = 20r_0$ and semimajor axis $a = 15r_0$. The units were chosen in such a way that $G = r_0 = M_{\rm tot} = 1$, where $M_{\rm tot}$ represents the total stellar mass involved in each merger simulation. A point mass representing the MBH was placed at the centre of each spherical system, with a mass $M_\bullet = 0.005M_{\rm g}$.

We performed three main groups of simulations, each characterized by a different inner slope for the colliding galaxies: $\gamma = 0.5$

Table 1. List of simulations. Column 1: simulation set (A, B, C); column 2: run name; column 3: total number of particles N; column 4: slope γ of the inner profile in each galaxy model. All mergers are equal mass.

Set	Run	N	γ
A	1	8k	0.5
	2	16k	0.5
	3	32k	0.5
	4	64k	0.5
	5	128k	0.5
	6	256k	0.5
	7	512k	0.5
	8	1M	0.5
B	1	8k	1.0
	2	16k	1.0
	3	32k	1.0
	4	64k	1.0
	5	128k	1.0
	6	256k	1.0
	7	512k	1.0
	8	1M	1.0
C	1	8k	1.5
	2	16k	1.5
	3	32k	1.5
	4	64k	1.5
	5	128k	1.5
	6	256k	1.5
	7	512k	1.5

Table 2. Parameters of the simulations. From left to right: initial semimajor axis, initial eccentricity, initial separation of the two original galaxies, scale radius of each galaxy, total stellar mass in each simulation, mass ratio between the two merging galaxies, mass ratio between the BHB and the stellar mass in the simulation, softening parameter.

a_i	e_i	Δr	r_0	M_{tot}	q	M_b/M_{tot}	ε
15	0.5	20	1	1	1	0.005	10^{-4}

for set A, $\gamma = 1$ for set B, and $\gamma = 1.5$ for set C. For each set, we considered different values for N from 8k to 1M. For set C the $N = 1$M case was avoided due to the prohibitively long integration time required. The list of performed simulations is given in Table 1. Each model was evolved for $t \approx 500$ time units; this choice ensures that the binary is followed for $\Delta t \gtrsim 100$ after the MBHs form a bound Keplerian pair. The parameters of the performed N-body experiments are summarized in Table 2.

The initial conditions were evolved adopting the integrator `HiGPUs`, a direct-summation N-body code based on the sixth-order Hermite scheme with block timesteps, designed to run on GPUs (Capuzzo-Dolcetta, Spera & Punzo 2013). The integrator adopts a Plummer softening kernel (Plummer 1911); we chose a softening parameter $\varepsilon = 10^{-4}$; this length scale is smaller than the minimum separation reached by the binary during its evolution. In `HiGPUs`, the individual particle timesteps are computed via a combination of the sixth- and fourth-order Aarseth criterion (Aarseth 2003; Nitadori & Makino 2008), and the two accuracy parameters were set equal to $\eta_{sixth} = 0.45$, $\eta_{fourth} = 0.01$ (for details, see Capuzzo-Dolcetta et al. 2013). The minimum and maximum possible values in the hierarchy of timesteps were chosen as $\Delta t_{min} = 2^{-29} \approx 1.863 \times 10^{-9}$ and $\Delta t_{max} = 2^{-6} = 0.015625$.

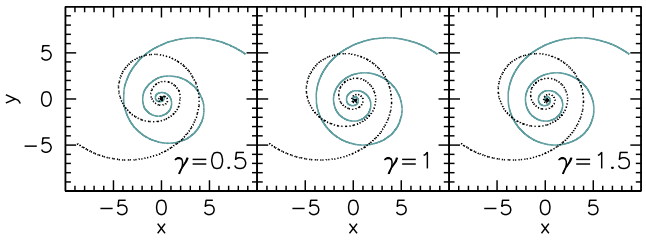

Figure 1. Trajectories of the two MBHs in the $x - y$ plane for the three sets of simulations, corresponding to $\gamma = 0.5$, 1.0, 1.5, from left to right, and $N = 512$k. In this figure and in the following, distances are in scalable N-body units.

All simulations of set A, B, and C were run allowing the BHB to wander (hereafter, *free-binary simulations*). Simulations of set B were then re-run while periodically re-centring the BHB at the centre of the merger remnant to quench the binary's wandering (hereafter, *fixed-binary simulations*).

3 SIMULATIONS AND BINARY EVOLUTION

The trajectories of the MBHs in the $x - y$ plane are shown in Fig. 1 for the three simulation sets. The initial evolution of the MBH pair reflects the orbit of the progenitor galaxies, which is the same for all three sets, and the trajectories are therefore quite similar. The time evolution of the binary separation is shown in Fig. 2, for the three different sets (free-binary simulations), and for $N = 512$k. This represents the maximum resolution available for all three γ values, and is therefore our fiducial resolution.

We can identify the typical three phases of BHB evolution in all our simulations. We consider an equal mass binary with total mass M_b. The first phase of evolution is driven by dynamical friction, which brings the MBH pair to a separation a_f, defined as the separation at which the stellar mass M_* enclosed in the binary orbit is twice the mass of the secondary MBH. In our case:

$$M_*(a_f) = M_b. \tag{2}$$

The time $t(a_f)$ at which this separation is reached approximately corresponds to the time of formation of a bound Keplerian binary in our equal mass simulations. Around this time, stellar encounters with stars on intersecting orbits start becoming important, and mark the beginning of the *strong three-body scattering regime* (Sesana 2010). In this phase, which sees a rapid shrinking of the binary separation, slingshot ejections first combine with dynamical friction and then become the main driver of binary hardening. This phase is rather short, and ends when the loss cone consisting of stars initially on intersecting orbits has been emptied. At this point, the inner cusp of the remnant is destroyed and a core has been carved in the stellar distribution.

We define the binary to be hard when its binding energy per unit mass exceeds the kinetic energy per unit mass of the field stars, i.e. when it reaches a separation

$$a_h = \frac{G\,M_b}{8\sigma_*^2}. \tag{3}$$

Here σ_* represents the velocity dispersion of the field stars (Milosavljević & Merritt 2001). From this moment, stars ejected from the nucleus via the slingshot mechanism attain a velocity greater than the escape velocity. The quantities a_f and a_h and their

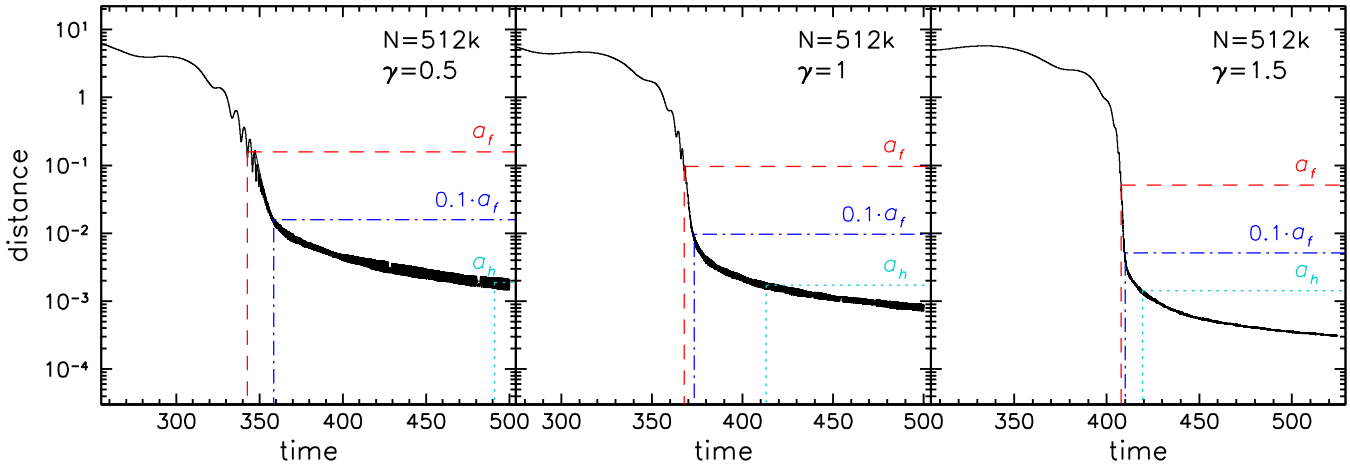

Figure 2. Evolution of the binary separation as a function of time for the runs with resolution $N = 512$k. From left to right, panels show the evolution for models with initial central density slope $\gamma = 0.5$, $\gamma = 1$ and $\gamma = 1.5$. The significant separations a_f (roughly at which the Keplerian binary forms, equation (2)), $a_f/10$ and a_h (from which slingshot interactions expel unbound stars, equation (3)) and their corresponding times are marked in the panels. In this figure and in the following, times and distances are in scalable N-body units.

corresponding times are marked in Fig. 2. The remnant mass distribution keeps memory of the initial slope γ, especially before the mass-carving has taken place; as a consequence, both a_f and a_h show a clear dependence on the initial value of γ (see Fig. 2): the radius containing the mass of the binary is smaller for merger products generated by steeper initial models, inducing a smaller a_f, while the velocity dispersion σ_*^2 of cuspier models is expected to be higher and produces a smaller a_h.

We also define the hardening rate

$$s(t) = \frac{\mathrm{d}}{\mathrm{d}t}\frac{1}{a}, \tag{4}$$

where a represents the semimajor axis of the binary. We compute s in all simulations by performing a linear fit to $a^{-1}(t)$ in small time intervals, and plot its time evolution in the middle panels of Fig. 3. The hardening rate is approximately constant with time. This behaviour is expected for binaries hardening in constant density backgrounds (Hills 1983), i.e. when the stellar field is unaffected by the binary evolution. Since this is not the case in a merger, the roughly constant nature of s implies that the loss cone is efficiently replenished, in agreement with previous studies that found the BHB to merge within a Hubble time (Khan et al. 2011; Preto et al. 2011; Gualandris & Merritt 2012).

The figure also shows the evolution of the inverse semimajor axis $1/a$ (top panels) and the number of stars inside the loss cone $N_{\rm lc}$, normalized to the total number of stars. Since hardening is assumed to be due to stars in the loss cone interacting with the binary, it is useful to monitor how many stars can be found in the loss cone at any given time. A star is considered to belong to the loss cone if its angular momentum per unit mass (L_*) is smaller than the angular momentum per unit mass of the binary, i.e. $L_* \leq L_{\rm b} = \sqrt{G\,M_{\rm b}\,a(1-e^2)}$. We find that after the binary has become hard, the fraction of stars in the loss cone is approximately constant, or only slightly decreasing, on the time-scale considered in the simulations. The decrease is due to the fact that the loss cone shrinks with time as the binary separation shrinks (Vasiliev et al. 2015).

4 BROWNIAN MOTION

4.1 Theoretical expectations

The Brownian motion of a single MBH in a nucleus is well described by a random walk due to encounters with field stars (Chandrasekhar 1942, 1943). If a massive object with mass M is surrounded by an isothermal distribution of stars, its velocity dispersion σ is expected to obey energy equipartition with the background stars:

$$\sigma^2 = \frac{m}{M}\sigma_*^2, \tag{5}$$

where σ_* is the stellar velocity dispersion and m is the typical stellar mass. This result has been shown to remain valid for a wide range of stellar backgrounds (Dorband, Hemsendorf & Merritt 2003; Merritt 2005; Merritt, Berczik & Laun 2007a). A similar behaviour is expected for the CoM of a BHB in a galactic nucleus. *Superelastic scattering* and the fact that stars are ejected in random directions slightly enhance the Brownian motion amplitude in the binary case; however, Merritt (2001) showed that the binary's random motion in phase space is dominated by distant encounters and therefore the wandering essentially obeys equation (5). Merritt (2001) derived an expression for the characteristic amplitude of the motion $r_{\rm b}$, under the assumptions that (i) the binary is placed in a constant density core, (ii) the stellar potential is harmonic and (iii) the Brownian motion has no influence on the stellar velocity field and mass distribution:

$$\begin{aligned} r_{\rm b} &= \left(\frac{R_2}{R_1}\right)^{1/2}\left(\frac{m}{M_{\rm b}}\right)^{1/2} r_{\rm c} \\ &= 0.01\,\mathrm{pc}\left(\frac{R_2}{R_1}\right)^{1/2}\left(\frac{m}{\mathrm{M}_\odot}\right)^{1/2}\left(\frac{10^8\,\mathrm{M}_\odot}{M_{\rm b}}\right)^{1/2}\left(\frac{r_{\rm c}}{100\,\mathrm{pc}}\right), \end{aligned} \tag{6}$$

where $(R_2/R_1)^{1/2}$ is a factor of order unity related to Chandrasekhar's coefficients, $r_{\rm c}$ represents the King core radius (King 1966) and $M_{\rm b}$ is the total mass of the binary.

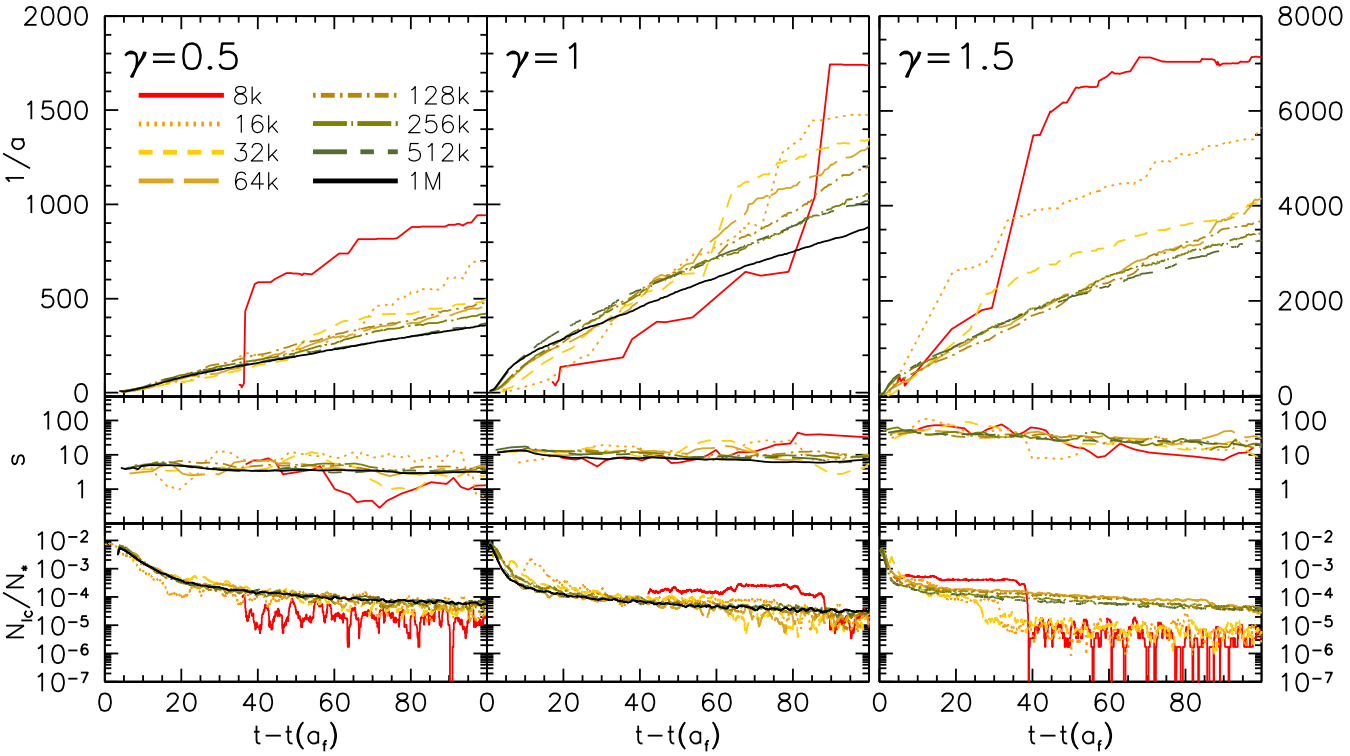

Figure 3. Time evolution of the inverse semimajor axis $1/a$ (top panels), hardening rate (middle panels) and fraction of loss cone stars (bottom panels) for all the available resolutions from $N = 8$k to $N = 1$M. We averaged the hardening rate over several time intervals, to smooth fluctuations. The left-hand panels refer to the set with initial density slope $\gamma = 0.5$, the central panels refer to the set with $\gamma = 1$ and the right-hand panels refer to the last set with $\gamma = 1.5$. Notice the different scale of the vertical axis in the top right panel. Time on the horizontal axis is given from the time corresponding to $a = a_f$.

4.2 Free-binary simulations

In order to characterize the Brownian motion of the BHB, it is necessary to define a meaningful reference position to be compared with the binary CoM over time. In principle, one could think of using the centre of mass of the whole stellar system, but this is dominated by the outermost stars which have a negligible influence on the BHB evolution. A better option is the centre of mass of the 50 per cent innermost stars in the system, which allows one to discard the outermost stars and consider only stars belonging to the density cusp to define the reference centre. Since at early times two stellar cusps are present, we started the Brownian motion characterization from the moment when the binary separation reaches $a_f/10$: at this stage, the Keplerian binary has formed and the two original systems have already merged into a single cusp.[2]

We evaluated the typical wandering radius of the binary in the following way: (i) first we computed the CoM (C0) from 50 per cent of the particles closest to the binary's CoM; (ii) then we reiterated the procedure by evaluating a more accurate CoM (C1) over the 50 per cent stars closer to C0, once this quantity is known. The displacement of C1 from the BHB CoM constitutes our best estimate of the binary wandering amplitude r_b over time. It is worth stressing that our recursive approach avoids biases induced by the selection of stars with respect to the position of the BHB.

[2] This particular moment has been chosen since it corresponds approximately to the point when the binary decay slows down considerably in all the three sets of simulations performed. We avoided other approaches due to the noisy trend of the binary separation in the lower-N cases.

The proportionality relation $\sigma^2 \propto m$ from equation (5) can be verified by computing the BHB CoM velocity dispersion σ^2 with respect to the CoM velocity of the stellar background σ_*. This velocity CoM has been computed over the same stars used for the calculation of C1.

In order to test the binary Brownian motion dependence on the number of particles in each simulation, we averaged the hardening rate s, binary wandering radius r_b and CoM velocity dispersion σ^2 over time from the moment at which the binary separation reaches $a_f/10$ and for Δt=100 time units. From equation (5), we expect a theoretical dependence of $r_b \propto N^{-0.5}$ and $\sigma^2 \propto N^{-1}$, given that $m = 1/N$ in the simulations. The averaged σ^2, r_b and s are shown in Fig. 4 as a function of N. We performed a power-law fit of the obtained data points for each of these quantities as a linear least-square fit in logarithmic scale. We thus obtained a dependence of the form $r_b \propto N^{p_r}$, $\sigma^2 \propto N^{p_{\sigma^2}}$ and $s \propto N^{p_s}$. The computed power-law indexes are listed in Table 3 and show a good agreement with the expected values $p_{\sigma^2} = -1$ and $p_r = -0.5$. Therefore the observed amplitude of the binary's Brownian motion follows the expected theoretical dependence on particle number.

If the loss cone refilling were driven by Brownian motion, a similar dependence on N would be expected for the hardening rate. However, this is not observed, and the hardening rate of the binary shows a much weaker dependence on N than the amplitude of the wandering. We argue that such dependence is due to a combination of collisional repopulation of the loss cone and Brownian motion at these moderate values of N, but should become

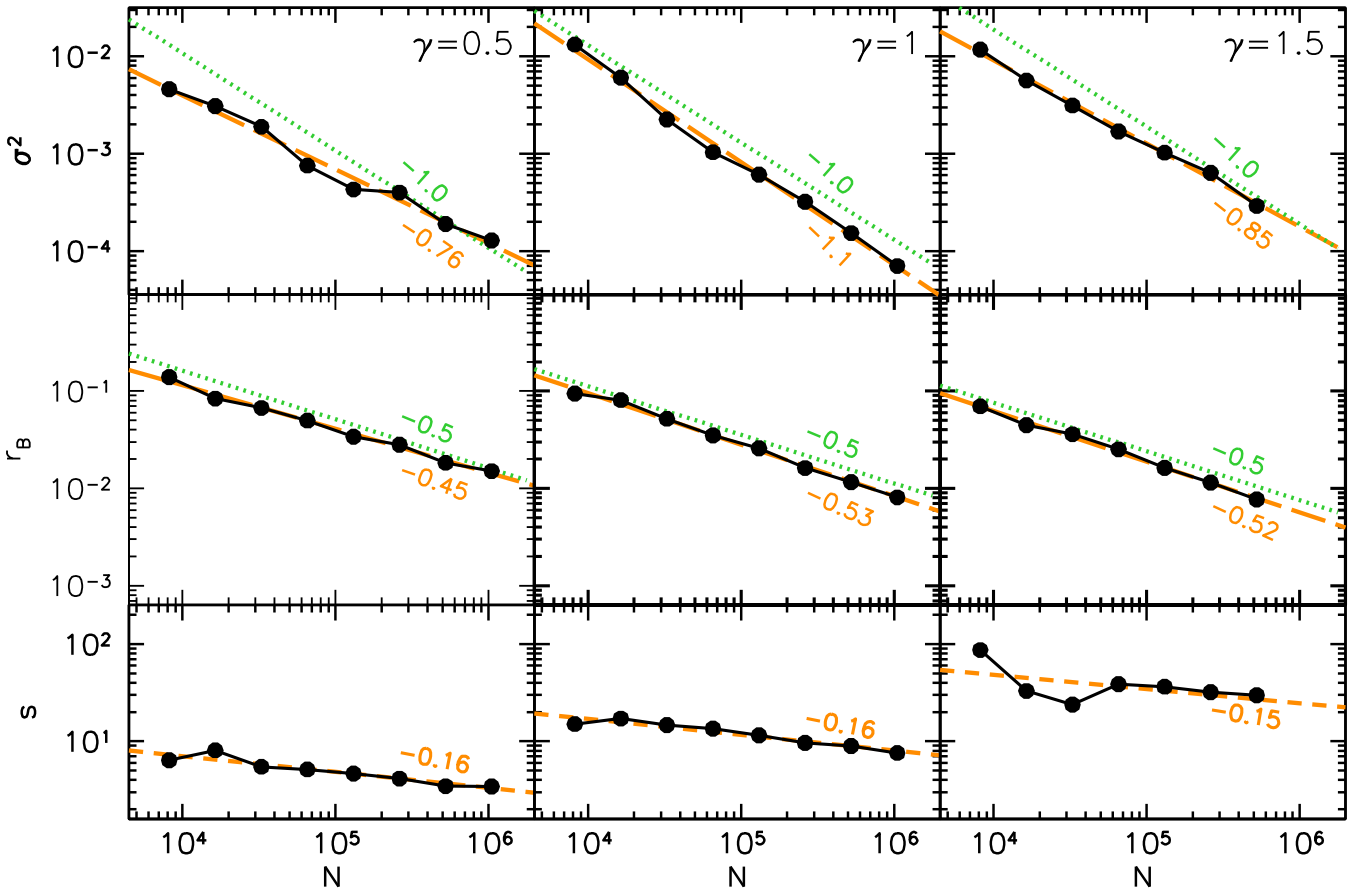

Figure 4. Analysis of the BHB Browninan motion. Top: time-averaged binary velocity dispersion as a function of the number of particles N in each simulation. Centre: time-averaged wandering radius of the BHB as a function of particle number. Bottom: time-averaged hardening rate versus particle number. In all cases, the average is computed from the time when a separation $a_f/10$ is reached and over 100 time units thereafter. The orange dashed lines represent power-law fits to the data and the obtained best-fitting slopes are given by the orange labels below the lines. The green dotted lines indicate the expected dependencies based on theoretical models, with slopes given by the green labels above the lines. In all cases, the left-hand panels refer to simulations with $\gamma = 0.5$, central panels refer to simulations with $\gamma = 1$, and right-hand panels to the set with $\gamma = 1.5$.

Table 3. List of best-fitting power-law indexes of the BHB CoM velocity dispersion (σ^2), wandering amplitude (r_b) and hardening rate (s). Column 1: index name; column 2: expected values based on theoretical arguments; columns 3–5: results for simulations whose initial galaxies had inner slope $\gamma = 0.5$, 1.0, 1.5, respectively.

Index	Exp.	$\gamma = 0.5$	$\gamma = 1$	$\gamma = 1.5$
p_{σ^2}	−1	−0.76	−1.1	−0.86
p_{r_b}	−0.5	−0.45	−0.53	−0.52
p_s	0	−0.16	−0.16	−0.15

negligible at more realistic particle numbers (Gualandris et al., in preparation).

4.3 Fixed-binary simulations

In order to draw a more robust conclusion about the role of Brownian motion in loss cone refilling, we re-ran the set of simulations with $\gamma = 1.0$ while periodically re-centring the binary at the centre of the merger remnant to quench the binary's wandering. To this purpose, we introduced the following modifications in the N-body integrator: (i) at each integration step, both MBHs were forced to advance with the smallest populated timestep in the hierarchy; (ii) the BHB was pinned down at the centre of the density cusp by shifting the binary CoM position during each corrector step and setting its velocity to zero. These new runs were started at the time when the binary separation in the original simulations drops below $a_f/10$. The centre of the stellar density cusp was evaluated by computing the CoM of particles inside a sphere with radius l_0 (≈5), i.e. the sphere containing 50 per cent of stars at the beginning of these new runs. During each corrector step the predicted positions of the stars were used to (i) estimate the CoM (S0) of particles within a distance l_0 from the binary CoM and (ii) reiterate the procedure by computing a more precise CoM (S1) using the just estimated CoM (S0) as new centre of the sphere. We refer to this new set of integrations as *fixed-binary* simulations, to distinguish them from the previous *free-binary* ones.

From Fig. 5 it is apparent that the hardening rate is lower for the fixed-binary runs in the low-N limit. As the resolution is increased, though, the free-binary evolution resembles more and more the fixed-binary evolution. This aspect can be better appreciated from Fig. 6: the time-averaged hardening rate in the free-binary runs approaches the hardening rate of the runs with anchored BHB as N increases, and the binary behaviour converges in the higher resolution simulations. Accordingly, the power-law dependence of the

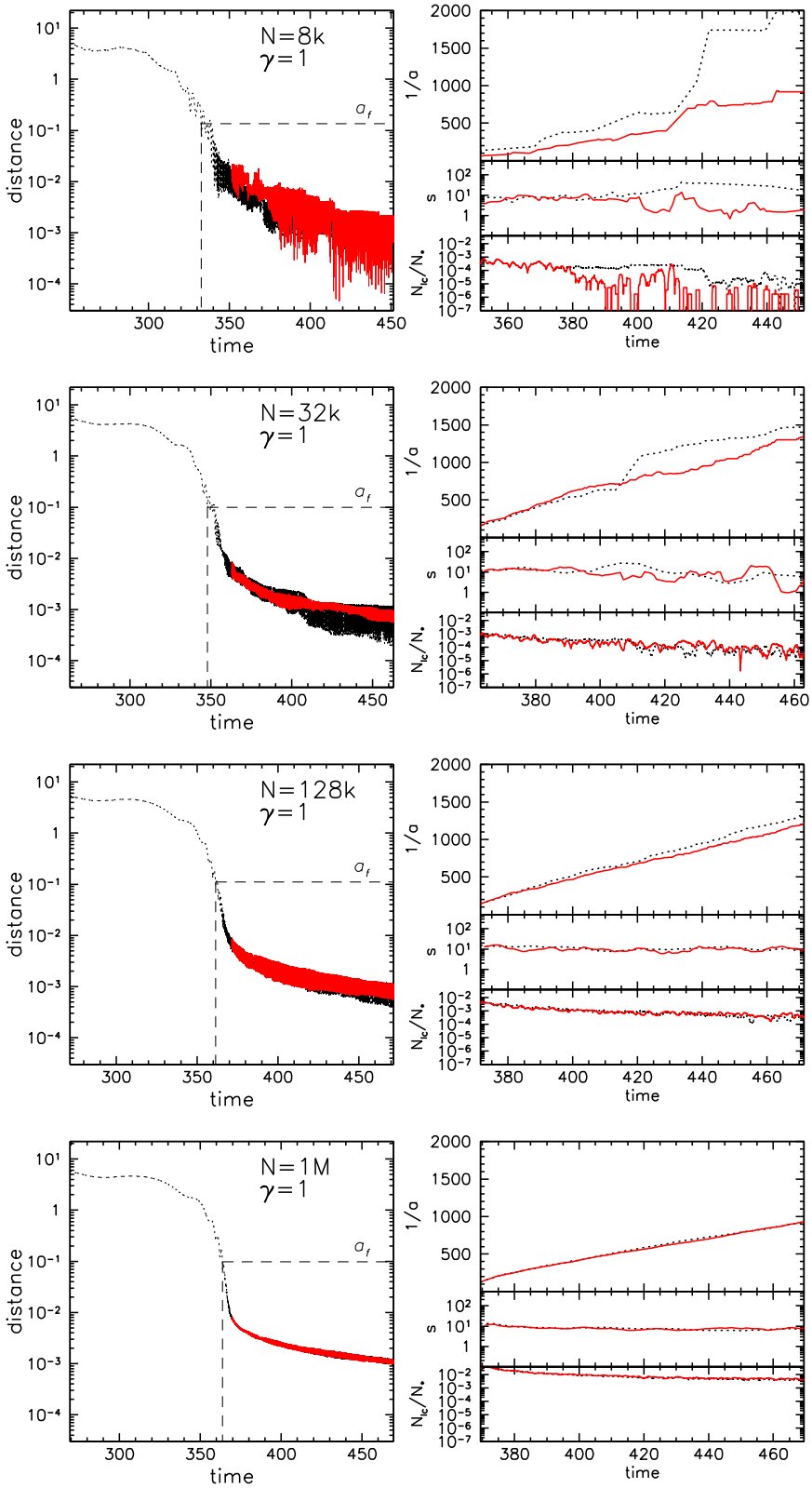

Figure 5. Evolution of the binary separation (left-hand panels) and of the inverse semimajor axis $1/a$, hardening rate s and fraction of loss cone stars $N_{\rm lc}/N$ (from top to bottom, right-hand panels). The free-binary evolution is shown with a black dotted line, while the fixed-binary evolution is overplotted with a red solid line. We present the evolution for some of the available resolutions: from top to bottom, $N = 8$k, 32k, 128k, 1M. All panels refer to the set of simulations with $\gamma = 1$.

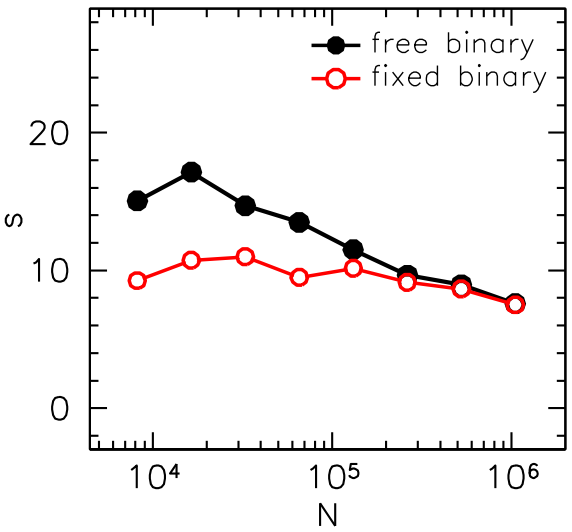

Figure 6. Time-averaged binary hardening rate as a function of the number of simulated particles for the $\gamma = 1$ set in the case of free-binary evolution (black filled circles) and fixed-binary evolution (red open circles). The two sets converge at the largest N values.

averaged hardening rate on N in the fixed-binary simulations is shallower ($p_s = -0.052$) compared to the one obtained from the free-binary runs ($p_s = -0.16$).

In addition, we note that the hardening rate measured in the low-N runs with fixed binary is only slightly larger than the same rate measured at the highest particle number. This implies that Brownian motion has a non negligible role in loss cone refilling for particle numbers in the range $10^4 \leq N \leq 10^6$, while it does not appreciably influence the BHB evolution if $N \gtrsim 10^6$.

Chatterjee et al. (2003) and Quinlan & Hernquist (1997) used a similar strategy and compared simulations in which the binary is free to wander with simulations in which the BHB CoM is pinned down at the origin; however they both find that hardening quickly stops after the first loss cone depletion if the binary is not allowed to random walk. This discrepancy comes from the fact that (i) Chatterjee et al. (2003) and Quinlan & Hernquist (1997) used a different integration technique with respect to our paper, and (ii) they simulated the BHB evolution in spherical systems, where triaxial loss cone refilling is inhibited; this mechanism is indeed expected to be the main driver of the BHB hardening in high-resolution runs.

We conclude that Brownian motion has an appreciable influence on the BHB evolution only at small particle numbers, and it can be safely neglected in free-binary simulations for $N \gtrsim 1$M.

5 SUMMARY

Massive BHBs are believed to form in the final stages of galaxy mergers. The formation of MBH pairs in gas-poor environments is driven by a combination of dynamical friction and close encounters with stars on low angular momentum orbits. However, both theoretical models and simulations show that evolution via the slingshot mechanism may be ineffective in bringing the binaries to coalescence if the loss cone region is not efficiently replenished. Recent simulations suggest that a departure from spherical symmetry in the merger remnant may lead to a change in the main mechanism driving loss cone refilling, from collisional two-body scatterings to collisionless torques in non-spherical systems. The reliability of these results may be questioned given the modest particle number achievable in current state-of-the-art direct-summation N-body simulations. In such cases, the inevitable wandering of the binary due to Brownian motion results in a larger population of stars on loss cone orbits.

In this work, we investigated the significance of Brownian motion of BHBs in merger simulations in the context of the final parsec problem. We performed three sets of direct-summation simulations corresponding to three different choices of the inner slope of the density profile ($\gamma = 0.5$, 1.0, and 1.5), and varying the particle number (from 8k to 1M particles).

We found that the effect of Brownian motion on the binary evolution is rather weak, and the Brownian motion amplitude r_b is in good agreement with the expected $r_b \propto N^{-0.5}$ relation, while the binary hardening rate only exhibits a weaker dependence on N.

We also performed additional simulations in which the binary centre of mass was fixed at the centre of the density cusp (fixed-binary runs), and we found that the hardening rate of the BHB measured in the free-binary and fixed-binary case converge to similar values for $N \sim$1M. Moreover, the hardening rate measured in low-N models with a fixed-binary evolution is only slightly larger than the one measured in high-N free-binary runs. This suggests that the role of Brownian motion in merger simulations is comparable to the effect collisional loss cone repopulation for $10^4 \lesssim N \lesssim 10^6$. However, Brownian motion is not important for $N \gtrsim 1$ M even in free-binary simulations.

Our findings support the general belief that non-sphericity of merger remnants leads to efficient collisionless loss cone refilling (Khan et al. 2011; Preto et al. 2011; Gualandris & Merritt 2012) and the final parsec problem disappears whenever this dominates over collisional effects.

ACKNOWLEDGEMENTS

We warmly thank Monica Colpi and Eugene Vasiliev for useful discussions and suggestions. We also thank the anonymous referee for their useful comments. The N-body integrations were carried out on the GPU cards *CUDA GeForce GTX 780*, *CUDA GeForce GTX 780 Ti* at the University of Surrey and on the *CUDA Tesla K80* GPUs hosted by the Italian supercomputing consortium *CINECA*. We would like to thank the Astrophysics group at the University of Surrey for the possibility of running most of the presented simulations. We acknowledge the CINECA Award N. HP10CP8A4R, 2016 for the availability of high performance computing resources and support. EB and MM acknowledge financial support from the Istituto Nazionale di Astrofisica (INAF) through a Cycle 31st PhD grant, from the Italian Ministry of Education, University and Research (MIUR) through grant FIRB 2012 RBFR12PM1F, from INAF through grant PRIN-2014-14, and from the MERAC Foundation.

REFERENCES

Aarseth S. J., 2003, Gravitational N-Body Simulations: Tools and Algorithms. Cambridge Univ. Press, Cambridge
Abbott B. P. et al., 2016, Phys. Rev. Lett., 116, 061102
Babak S. et al., 2016, MNRAS, 455, 1665
Begelman M. C., Blandford R. D., Rees M. J., 1980, Nature, 287, 307
Berczik P., Merritt D., Spurzem R., 2005, ApJ, 633, 680
Capuzzo-Dolcetta R., Spera M., Punzo D., 2013, J. Comput. Phys., 236, 580
Chandrasekhar S., 1942, Principles of Stellar Dynamics. Dover Publications Inc., New York
Chandrasekhar S., 1943, ApJ, 97, 255
Chatterjee P., Hernquist L., Loeb A., 2003, ApJ, 592, 32

Dehnen W., 1993, MNRAS, 265, 250
Dorband E. N., Hemsendorf M., Merritt D., 2003, J. Comput. Phys., 185, 484
eLISA Consortium 2013, The Gravitational Universe, the science theme selected by ESA as L3 mission, preprint (arXiv:1305.5720)
Ferrarese L., Ford H., 2005, Space Sci. Rev., 116, 523
Gualandris A., Merritt D., 2012, ApJ, 744, 74
Haehnelt M. G., Rees M. J., 1993, MNRAS, 263, 168
Hills J. G., 1983, AJ, 88, 1269
Khan F. M., Just A., Merritt D., 2011, ApJ, 732, 89
King I. R., 1966, AJ, 71, 64
Makino J., Funato Y., 2004, ApJ, 602, 93
Merritt D., 2001, ApJ, 556, 245
Merritt D., 2005, ApJ, 628, 673
Merritt D., Berczik P., Laun F., 2007a, AJ, 133, 553
Merritt D., Mikkola S., Szell A., 2007b, ApJ, 671, 53
Milosavljević M., Merritt D., 2001, ApJ, 563, 34
Milosavljević M., Merritt D., 2003, ApJ, 596, 860
Nitadori K., Makino J., 2008, New Astron., 13, 498
Plummer H. C., 1911, MNRAS, 71, 460
Preto M., Berentzen I., Berczik P., Spurzem R., 2011, ApJ, 732, L26
Quinlan G. D., Hernquist L., 1997, New Astron., 2, 533
Saslaw W. C., Valtonen M. J., Aarseth S. J., 1974, ApJ, 190, 253
Sesana A., 2010, ApJ, 719, 851
Thorne K. S., Braginskii V. B., 1976, ApJ, 204, L1
Vasiliev E., Antonini F., Merritt D., 2015, ApJ, 810, 49
Volonteri M., 2010, A&AR, 18, 279
Yu Q., 2002, MNRAS, 331, 935

This paper has been typeset from a TEX/LATEX file prepared by the author.